Effect of Collisionless Heating on Electron Energy Distribution in an Inductively Coupled Plasma

Valery A. Godyak
OSRAM SYLVANIA Development Inc., 71 Cherry Hill Drive, Beverly, Massachusetts 01915

Vladimir I. Kolobov
CFD Research Corporation, 215 Wynn Drive, Huntsville, Alabama 35805
(Received 23 March 1998)

Significant frequency dependence of the electron energy distribution has been found in a low-pressure inductive discharge experiment. The observed frequency dependence reveals the presence of collisionless electron heating and appears as a result of finite electron-transit time through the skin layer. The energy distributions calculated from a kinetic equation accounting for nonlocality of electron kinetics and electrodynamics are in good agreement with the experiment. [S0031-9007(98)06549-1]

PACS numbers: 52.80.–s, 52.65.–y

The recent advent of high density plasma sources sustained by radio-frequency (rf) electromagnetic fields at low gas pressure has raised significant interest in electron heating and plasma maintenance in the near-collisionless regime where the electron mean free path λ is comparable to or larger than plasma dimensions. In contrast to a collisionally dominated plasma with Joule heating, electron heating in the near-collisionless plasma is a combined effect of electron interactions with electromagnetic fields, reflections from plasma boundaries, and collisions with gas particles [1–3]. The penetration of electromagnetic energy into such a plasma exhibits peculiarities typical to the anomalous skin effect [4–6]. Nonmonotonic distributions of the rf fields and current density [7], collisionless electron heating [8], and negative power absorption [9] have recently been observed in experiments with low pressure inductive plasmas and reviewed in Ref. [10]. In this Letter we report on a significant frequency dependence of the electron energy distribution function (EEDF) found in experiments with inductively coupled plasma (ICP) at low gas pressure. According to the developed theory, the frequency dependence of the EEDF is associated with finite electron transit time through the skin layer.

The experiments were carried out in a cylindrical ICP maintained by a planar inductor coil in a stainless steel chamber with a quartz bottom. Details of the experimental setup are published elsewhere [7,9,10]. Briefly, the chamber ID was 19.8 cm, its length L was 10.5 cm, and the quartz thickness was 1.27 cm. A five turn planar induction coil was mounted 1.9 cm below the bottom surface of the discharge chamber. An electrostatic shield between the quartz and the coil has practically eliminated capacitive coupling between the induction coil and plasma to the extent that the rf plasma potential referenced to the grounded chamber was much less than 1 V. That made it possible to resolve the low energy part of the measured EEDF previously not detected in all published experiments carried out in ICP's. A noise supression circuit with an additional reference probe [11] has extended the dynamic range of the EEDF measurement up to 3–4 orders of magnitude and enabled us to resolve electrons with energy far beyond the excitation and ionization thresholds of argon atoms. Measurements were made at driving frequencies $\omega/2\pi = 3.39$, 6.78, and 13.56 MHz in an argon discharge at gas pressures of 1 and 10 mTorr and discharge power P_{pl} in a range of 12–200 W. The power dissipated in the plasma, P_{pl}, was determined by measuring the power transmitted to the inductor coil (forward minus reflected power) and subtracting matcher and coil losses determined *a priori* as a function of coil current and temperature.

Results of Langmuir probe measurement performed in the discharge center ($r = 0$ and $z = 5$ cm) are shown in Fig. 1 for different ω and P_{pl}. Here the electron energy distribution is given in terms of the electron energy probability function (EEPF) measured by Langmuir probe. The plasma parameters found as corresponding integrals of the measured EEPF: the electron density n_e, the effective electron temperature T_{eff}, and the electron-atom transport collision frequency ν_m in rf field are given in Table I together with the rms electric field E_0 near the quartz window (at $r = 4$, $z = 0$ cm) measured in Ref. [7]. The observed EEPF's are non-Maxwellian and in general have a three temperature structure. There is a group of low energy electrons with temperature $T_e(\varepsilon) = (d \ln f_0/d\varepsilon)^{-1}$ less than the effective temperature T_{eff} of the EEPF, similar to that found in capacitive rf discharges [12]. There is also a EEPF depletion (compared to Maxwellian) at energies higher than 12 eV due to excitation and ionization of argon atoms by electron impact. Substantial changes of the EEPF slope with frequency observed at energies close to average ones (see Fig. 1) correspond to changing of the effective electron temperature shown in Table I. The frequency dependence is well pronounced at lower plasma densities (power) and gradually vanishes at higher densities where Coulomb interactions among electrons

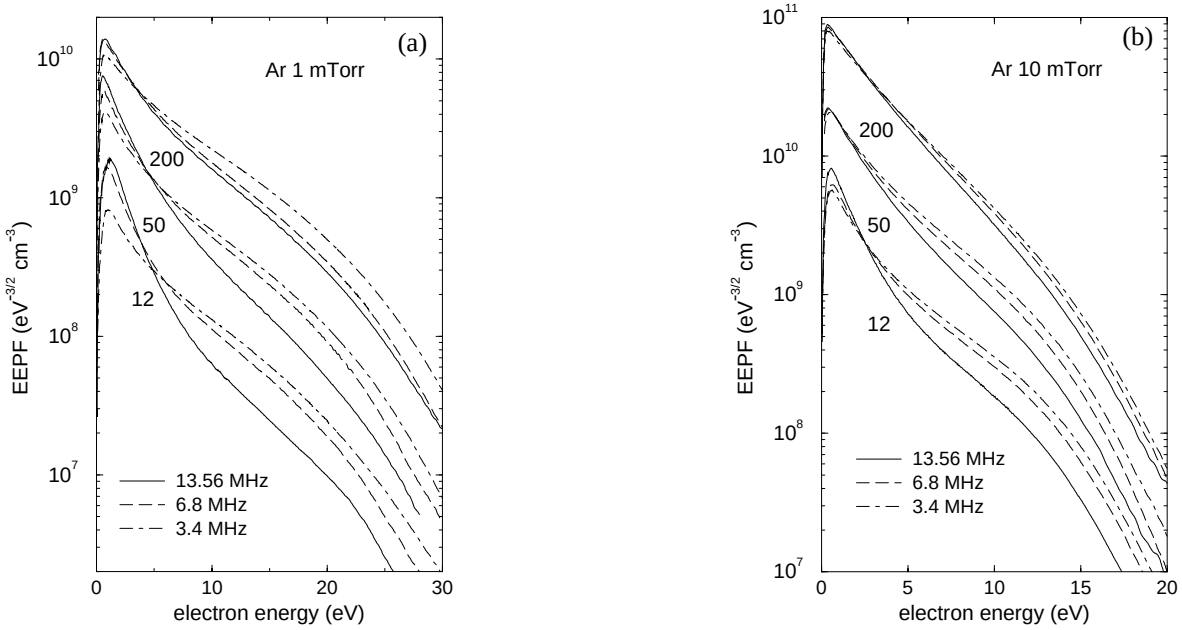

FIG. 1. Measured EEPF's for 1 and 10 mTorr.

tend to maxwellize the EEPF in the elastic energy range. No frequency dependence of plasma density was found in this experiment.

The EEPF was calculated from the kinetic equation

$$\frac{1}{\langle v\rangle}\frac{d}{d\varepsilon}\langle v\rangle \mathcal{D}_E \frac{df_0}{d\varepsilon} = S\,, \tag{1}$$

where ε is the total electron energy (kinetic plus potential), $\langle v\rangle$ denotes the electron velocity averaged over the discharge volume accessible to electrons with total energy ε, and $\mathcal{D}_E$ is the energy diffusion coefficient which describes electron heating. The term S on the right hand side accounts for energy transfer in Coulomb interactions among electrons and inelastic collisions of electrons with argon atoms [13].

The energy diffusion coefficient $\mathcal{D}_E(\varepsilon)$ has recently been calculated for some limiting cases in [2,3,14]. Here we extend these results by accounting for elastic collisions and peculiarities of the rf field profile in the two-dimensional system studied in the experiment [7]. Taking into consideration thermal electron motion in the axial direction, assuming a spatially homogeneous plasma and an azimuthal electric field in the form $E_\theta(r,z) = E_0 J_1(3.8r/R)E(z)$ (J_1 is the Bessel function), we found

$$\mathcal{D}_E = D_0 \sum_{n=-\infty}^{\infty} |E_n|^2 \Psi\left(\frac{k_n v}{\omega}, \frac{\nu}{\omega}\right), \tag{2}$$

where $D_0 = \kappa\varepsilon\varepsilon_0\omega$, $\varepsilon_0 = (eE_0/2\omega)^2/m$ is a characteristic energy, $\nu(\varepsilon)$ is the transport collision frequency (a function of electron energy), $\kappa \approx 0.3$ is a result of E_θ averaging over the radial coordinate, E_n is the Fourier spectrum of $E(z)$, and $k_n = \pi n/L$. Heating results from electron interactions with all components of the field spectrum and the function

TABLE I. Experimental data for electron density n_e, effective electron temperature T_{eff}, and collision frequency ν_m in the discharge center ($z = 5$, $r = 0$ cm) and the rms electric field E_0 at $z = 0$, $r = 4$ cm for different power P_{pl}, driving frequency f, and argon pressure p.

p (mTorr)		1	10	1	10	1	10	1	10
P_{pl} (W)	f (MHz)	$n_e \times 10^{10}$ (cm^{-3})		T_{eff} (eV)		$\nu_m \times 10^6$ (s^{-1})		E_0 (V/cm)	
	3.39			5.3	3.4	7.8	55	1.9	1.4
12	6.78	1.0	2.8	4.2	3.1	7.4	58	2.1	1.6
	13.56			2.9	2.5	6.1	50	3.5	2.2
	3.39			5.4	3.3	7.9	53	2.1	1.5
50	6.78	4.1	11	4.7	3.1	7.6	56	2.4	1.8
	13.56			3.7	2.8	6.9	53	4.0	2.5
	3.39			6.0	3.1	8.1	51	2.2	1.7
200	6.78	13	43	5.2	3.0	7.7	52	2.8	2.0
	13.56			5.0	2.8	7.6	52	4.4	3.0

$$\Psi(x,y) = x^{-3}\left\{(x^2 + y^2 - 1)\left[\arctan\frac{1+x}{y} - \arctan\frac{1-x}{y}\right] - 2xy + y\ln\left[\frac{y^2 + (1+x)^2}{y^2 + (1-x)^2}\right]\right\} \quad (3)$$

describes the contribution of different spectral components.

In limiting cases, Eq. (2) reproduces well-known results. In a cold plasma (at $k\upsilon/\omega \ll 1$, k is a typical wave number) all modes give equal contribution, $\Psi(0,y) = (4/3)y/(1+y^2)$, and the energy diffusion coefficient $\mathcal{D}_E$ corresponds to a spatially averaged Joule heating produced by an inhomogeneous rf electric field [15]:

$$\mathcal{D}_E = \frac{e^2\langle E_\theta^2\rangle \upsilon^2 \nu}{6(\omega^2 + \nu^2)}, \quad (4)$$

where

$$\langle E_\theta^2\rangle = \kappa E_0^2 \sum_{n=-\infty}^{\infty} |E_n|^2 = \frac{\kappa E_0^2}{L}\int_0^L |E|^2 dz \quad (5)$$

is the mean square of $E_\theta(r,z)$ averaged over discharge volume.

In a warm plasma, the zero component of the spectrum (which corresponds to a spatially uniform electric field) gives no contribution to the collisionless heating since $\Psi(0,\nu/\omega) \propto \nu$. For $\nu/\omega \ll 1$, $\Psi(x,0) = \pi(x^2 - 1)/x^3$ at $x > 1$ and vanishes for slow electrons with $\upsilon < \omega/k$ [2]. A pronounced maximum at $x = \sqrt{3}$ indicates predominant heating of electrons with velocities close to transit-time resonance $\omega\tau \approx 1$, where $\tau = (k\upsilon_z)^{-1}$ is a characteristic time electrons spend in the region of inhomogeneous rf field (skin layer) [16]. The factor $\sqrt{3}$ appears as a result of averaging over velocity direction for an isotropic velocity distribution.

In our calculations, we used the Fourier spectrum E_n for a warm plasma slab [5]

$$E_n = \frac{2i\omega l^2 B_0}{LcE_0}\frac{[1 - \xi\cos\pi n]}{D(k_n l)}, \quad (6)$$

where $\xi = B_L/B_0$ is the ratio of the rf magnetic field amplitude at the boundaries [17]

$$\xi = \sum_{n=0}^{\infty}{}'(-1)^n D^{-1}(k_n l) \Big/ \sum_{n=0}^{\infty}{}' D^{-1}(k_n l) \quad (7)$$

and primes indicate that the term $n = 0$ is multiplied by $1/2$. The function $D(q)$ for a high density Maxwellian plasma is given by

$$D(q) = q^2 + \Lambda Z(is/q)/q + (3.8l/R)^2, \quad (8)$$

where the last term accounts for radial inhomogeneity of the rf electric field, and the nonlocality parameter

$$\Lambda = \left(\frac{\omega_p \upsilon_{\rm th}}{c}\right)^2 \frac{\omega}{(\omega^2 + \nu^2)^{3/2}} \quad (9)$$

describes the nature of the skin effect (anomalous for $\Lambda > 1$ and normal at $\Lambda < 1$). Here, ω_p is the electron plasma frequency, $s = i\exp[-i\arctan(\nu/\omega)]$ is a measure of plasma collisionality, $l = \upsilon_{\rm th}/\sqrt{\omega^2 + \nu^2}$ is an effective mean free path for an electron with the most probable speed $\upsilon_{\rm th} = (2T_e/m)^{1/2}$, and $Z(x)$ is the plasma dispersion function [18].

To analyze the influence of the finite size of the plasma, we performed calculations of the energy diffusion coefficient and EEPF for different gap lengths L_0. Figure 2 shows function $\eta(\varepsilon) = (L_0/L)\sum_{n=-\infty}^{\infty}|E_n|^2\Psi_n$ which corresponds to a dimensionless energy diffusion coefficient. Solid lines are for $L_0 = L$; dashed lines are for $L_0 = 4L$. At 10 mTorr, the frequency and energy dependencies of $\eta(\varepsilon)$ and $\mathcal{D}_E(\varepsilon)$ are well described by Eq. (4). In this case, changing the gap length does not result in any changes in the slope of $\eta(\varepsilon)$. At 1 mTorr, changes in the slope of $\eta(\varepsilon)$ at energies $\varepsilon_n = m(\omega L/\pi n)^2/2$ correspond to input of different harmonics in the series (2). Since E_n decays rapidly with an increase of n, the main contribution to heating comes from the first spatial harmonic of the field. At $\upsilon < \omega L/\pi$, only higher harmonics contribute to the heating and $\eta(\varepsilon)$ is small. The finite size of the plasma results also in some reduction of heating for high-energy electrons [2]. Although the size of the plasma affects the slope of $\eta(\varepsilon)$ at 1 mTorr, the EEPF shape is affected to a much lesser degree.

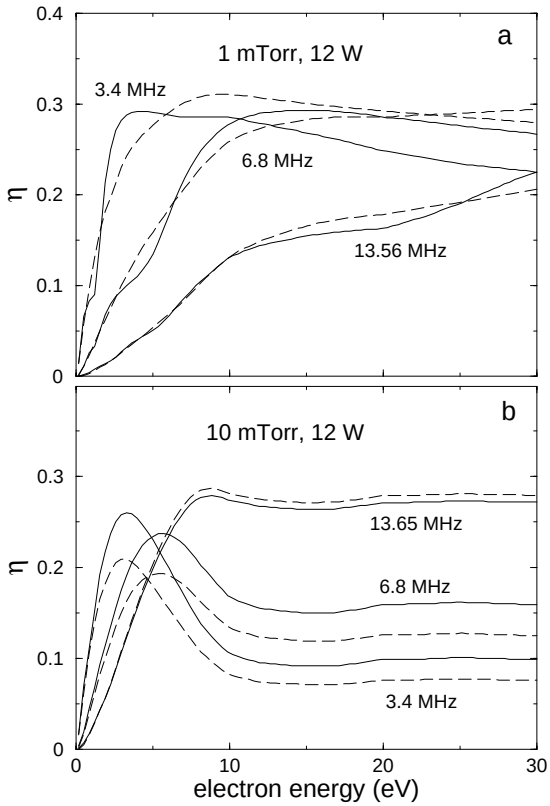

FIG. 2. The function $\eta(\varepsilon)$ calculated from (2). Solid lines are for the gap length $L_0 = 10.5$ cm; dashed lines are for $L_0 = 42$ cm.

The calculated EEPF's are shown in Fig. 3. Input parameters are taken from Table I; cross section data for electron collisions in argon are from [19]. The results of calculations are in good agreement with experiment in spite of the assumption of a homogeneous plasma and neglect of transverse electron motion in calculations. Accounting for the ambipolar electric field should enhance the low energy peak of the EEPF [20] and slightly change the energy corresponding to bounce resonances. The thermal electron motion in the transverse direction can further decrease the magnitude of bounce resonance effects.

There are several mechanisms which determine the shape of the EEDF in low pressure ICP's. They are as follows: (i) dependence of the collision frequency on electron energy (e.g., due to the Ramsauer effect), (ii) the presence of ambipolar potential which prevents slow electrons from entering the region of high rf field near the boundaries, (iii) the finite transit-time effect, and (iv) the bounce resonance effect. The first two do not depend on driving frequency. The last ones contain the frequency dependence that has been analyzed in the present work. Our studies indicate that bounce resonances due to the finite size of the plasma are not significant and that the observed frequency dependence of the EEDF is mainly due to finite electron transit time through the skin layer (in general, the region of inhomogeneous rf field). To the authors' knowledge, the present work is the first direct evidence of the collisionless heating effect on the EEDF shape in a weakly collisional ICP.

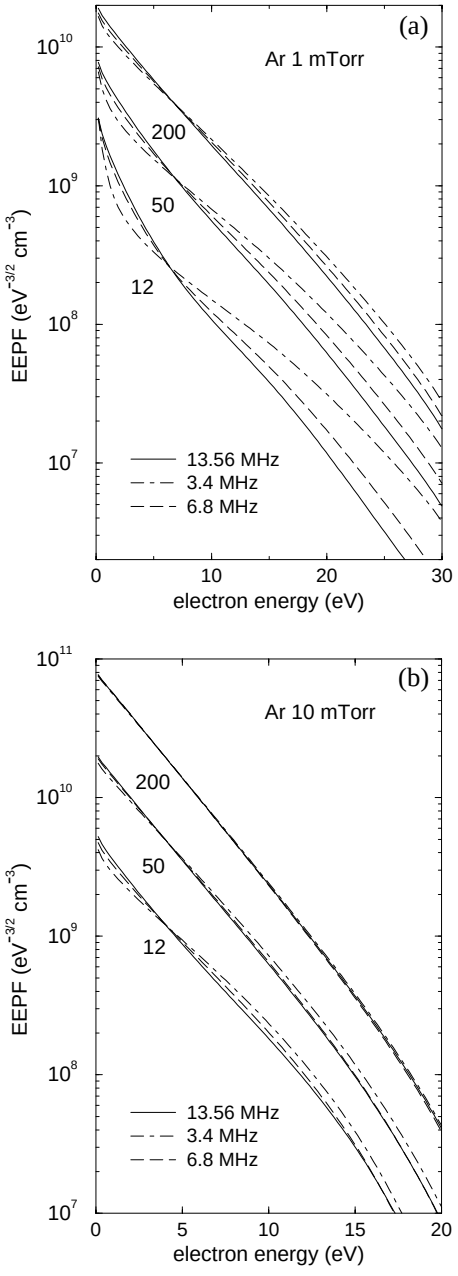

FIG. 3. Calculated EEPF's for experimental conditions of Fig. 1.

The authors thank R. B. Piejak and B. M. Alexandrovich for their valuable contributions to the experimental part of this work.

[1] I. D. Kaganovich, V. I. Kolobov, and L. D. Tsendin, Appl. Phys. Lett. **69**, 3818 (1996).
[2] Yu. M. Aliev, I. D. Kaganovich, and H. Schluter, Phys. Plasmas **4**, 2413 (1997).
[3] V. I. Kolobov, D. P. Lymberopoulos, and D. J. Economou, Phys. Rev. E **55**, 3408 (1997).
[4] E. S. Weibel, Phys. Fluids **10**, 741 (1967).
[5] V. I. Kolobov and D. J. Economou, Plasma Sources Sci. Technol. **6**, R1 (1997).
[6] N. S. Yoon, S. M. Hwang, and D.-I. Choi, Phys. Rev. E **55**, 7536 (1997).
[7] V. A. Godyak and R. B. Piejak, J. Appl. Phys. **82**, 5944 (1997).
[8] V. A. Godyak, R. B. Piejak, B. M. Alexandrovich, and V. I. Kolobov, Phys. Rev. Lett. **80**, 3264 (1998).
[9] V. A. Godyak and V. I. Kolobov, Phys. Rev. Lett. **79**, 4589 (1997).
[10] V. A. Godyak, in *Electron Kinetics in Glow Discharges*, edited by U. Kortschagen and L. D. Tsendin (Plenum Press, Inc., New York, 1998).
[11] V. A. Godyak, R. B. Piejak, and B. M. Alexandrovich, Plasma Sources Sci. Technol. **1**, 36 (1992).
[12] V. A. Godyak and R. B. Piejak, Phys. Rev. Lett. **65**, 996 (1990).
[13] V. I. Kolobov and W. N. G. Hitchon, Phys. Rev. E **52**, 972 (1995).
[14] R. H. Cohen and T. D. Rognlien, Plasma Sources Sci. Technol. **5**, 442 (1996).
[15] Yu. R. Alanakyan, Sov. J. Plasma Phys. **5**, 504 (1979).
[16] V. Vahedi *et al.*, J. Appl. Phys. **78**, 1446 (1995).
[17] A. N. Kondratenko, *Field Penetration into Plasmas* (Atomizdat, Moscow, 1979) (in Russian).
[18] B. D. Fried and S. D. Conte, *The Plasma Dispersion Function* (Academic Press, New York, 1961).
[19] A. Phelps, ftp://jila.colorado.edu/collision-data.
[20] U. Buddemeier, U. Kortschagen, and I. Pukropski, Appl. Phys. Lett. **67**, 191 (1995).